

GaAsSbP QUASITERNARY MATERIAL SYSTEM: NANOSTRUCTURES GROWTH FEATURES AND IMMISCIBILITY ANALYSIS

K. M. Gambaryan, A. K. Simonyan, V. M. Aroutiounian

Center of Semiconductor Devices and Nanotechnologies, Yerevan State University, Yerevan, Armenia

Received 5 September 2012

Abstract–The continuum elasticity model is applied to quantitatively investigate the growth features and nucleation mechanism of quantum dots (QDs), nanopits, and cooperative QDs–nanopits structures in GaAsSbP quasiternary systems. We determine the critical lattice mismatch of GaAs/GaAsSbP system equal to $\varepsilon = 0.03$, when the growth mode changes from nucleation of QDs to formation of nanopits. We show that the island's total energy and volume for that system are decreasing with increasing of the strain. The free energy of mixing for GaAs_{1-x-y}Sb_xP_y quasiternary system is calculated and studied and its 3D sketch is plotted. It is demonstrated that there are some immiscibility gap for that system, which strongly depends on temperature.

Keywords: continuum elasticity; GaAsSbP; quantum dots; nanopits

1. Introduction

The most promising from the point of view of designing new materials and devices with unique properties is at present elaboration of technologies for creation of novel semiconductor nanostructures and study of their physical properties. Steadily increasing interest towards specifically semiconductor nanostructures is caused primarily by the existence of a wide spectrum of possibilities to control the properties of semiconductors. It is known that crucial changes in their properties may be achieved by varying the composition of semiconductor solid solutions, changing the concentration and type of impurities, changing external conditions, and so on. Constraints of motion of charge carriers in one or more directions leading to the dimensional quantization phenomenon open additional possibilities of efficient control of properties of nanostructure-based devices by means of changing their sizes [1-4]. Modified density of states of quantum dots (QD), nanowires, and combined QD–nanopit structures leads to essential improvement of the working optoelectronic parameters of semiconductor devices, such as lasers, photodetectors, etc. Obviously, the electronic properties of QDs depend on dot structure and the mechanism of their formation. Such nanostructures can be fabricated by nanolithography or by the self-organization method (Stranski–Krastanov mode), which is at present the most frequently employed technique. Relaxation of elastic (deformation) strain as a principle of nucleation is the basic mechanism of formation of nanostructures in semiconductor materials such as Si, Ge, III-V compounds, etc.

The electronic properties of GaAs, GaSb and GaP suggest that the previously observed InAsSbP type II nanostructure [3,4] can be transformed into a type I system by replacing In with Ga, where both the electron and the hole states are localized inside the QD [5]. It recommends these structures for the near-IR light emission and other important devices. At nanostructures engineering

GaAsSb alloy is also used as a cap layer for the strain reduction particularly in InAs/GaAs QD system due to strain, induced Sb migration to the top of the InAs QDs, together with a transition to a type II band alignment [6]. GaAs_{1-x}P_x is a wide-band gap alloy that is successfully employed in red and green LEDs fabrication. This alloy remains a direct gap material in the composition range of $0 < x < 0.4$ at room temperature, but above $x = 0.48$ becomes indirect. The GaAsSbP quaternary epitaxial films previously have been successfully grown on a GaAs substrate by liquid phase epitaxy [7,8], electroepitaxy [9] and other technological techniques. GaSb QDs have been successfully grown on GaAs (001) substrate [10]. But application of GaAsSbP alloy for the growth of nanostructures has not been reported yet. Actually, very large difference in the respective diameters of the V elements (0.98 Å (P), 1.19 Å (As) and 1.38 Å (Sb)) and monitoring the composition ratio between As, Sb and P could lead to strain control (positive or negative comparing with GaAs substrate) in GaAsSbP leading to QDs, nanopits or QD/nanopits cooperative structures formation. But because the atoms mixing in GaAsSbP quaternary alloy occurs on the same arsenic sublattice, the system can exhibit the mixing problem and immiscibility gap (decomposition of solid solution) can be revealed at high concentrations of the antimony and phosphorus like in InAsSbP material system [4].

In this paper the continuum elasticity model is applied to quantitatively investigate the growth features and nucleation mechanism of QDs, nanopits, and cooperative QDs–nanopits structures in GaAsSbP quasiternary systems. The immiscibility analysis for that system is performed.

2. Quantum Dots–Pits Competing Nucleation Mechanisms in Strain-Induced GaAsSbP System

At the description of the competing nucleation mechanism we assume that the surface has only discrete orientations and that only one angle need be considered [11], so GaAsSbP-based QDs and nanopits have a shape as it is shown in Fig. 1. [12]

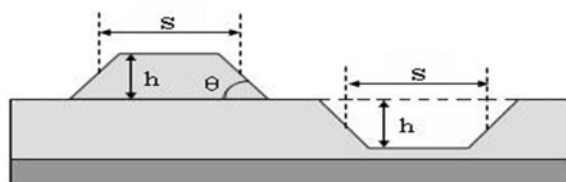


Fig. 1. Schematic view of the cross section of shape assumed for dot and pit.

The total free energy to form either a dot or a pit is $E = E_S + E_R$, where E_S and E_R are the change in surface free energy and the reduction of the strain energy by elastic relaxation, respectively. Minimizing the total free energy [11] with respect to shape for fixed volume gives $s = t = h \cot \theta$, where s , t , h and θ are the length, width, height (depth) and contact angle, as in Fig. 1. The energy is equal to

$$E = 4\Gamma V^{2/3} \tan^{1/3}\theta - 6cV \tan\theta, \quad (1)$$

where $\Gamma = \gamma_e \csc\theta - \gamma_s \cot\theta$. For the crystals with a cubic symmetry $\gamma_s = (1/2)\varepsilon^2 (C_{11} + C_{44})d_{wet}$, $c = \sigma_b^2(1-\nu)/2\pi\mu$, $\sigma_b = \varepsilon(C_{11} + C_{44})$ [12]. Here γ_s and γ_e are the surface free energy per unit area for the normal orientation and the beveled edge, respectively, $\varepsilon = \Delta a/a$ is the lattice mismatch ratio (strain) and d_{wet} is the wetting layer thickness. $\nu = \lambda/(2(\lambda + \mu))$ is the Poisson ratio, μ , λ and C_{ij} are the shear (Lame coefficients) and the elastic modulus of the substrate. Taking into account also the dependence of the wetting layer thickness versus strain, the expression for the total energy can be written as [12]

$$E = 4\left(\gamma_e \csc\theta - \frac{1}{2}\varepsilon^2 (C_{11} + C_{44})ae^{-35.84\varepsilon} \cot\theta\right)V^{2/3} \tan^{1/3}\theta - 3\varepsilon^2 (C_{11} + C_{44})^2 \frac{(1-\nu)}{\pi\mu}V \tan\theta. \quad (2)$$

In order to obtain analytical expression for the deformation dependence of wetting layer thickness in the case of the GaAsSbP quasiternary system, we performed mathematical approximation of experimental data. Approximation curves are presented in Fig. 2. We used in our calculations the following expressions for d_{wet} : in monolayers (ML): (i) if the deformation strain is positive, then $d_{wet} = 0.05\varepsilon^{-3/2}$ at $\varepsilon > 0.03$ [13] and $d_{wet} = 24.181e^{-31.034\varepsilon}$ at $0 < \varepsilon < 0.03$ (accuracy of approximation $R^2 = 0.9635$), (ii) if the deformation strain is negative, then $d_{wet} = 0.15|\varepsilon|^{-3/2}$ at $|\varepsilon| > 0.035$ [13] and $d_{wet} = 45.162e^{-23.03|\varepsilon|}$ at $0 < |\varepsilon| < 0.035$ (accuracy of approximation $R^2 = 0.9934$).

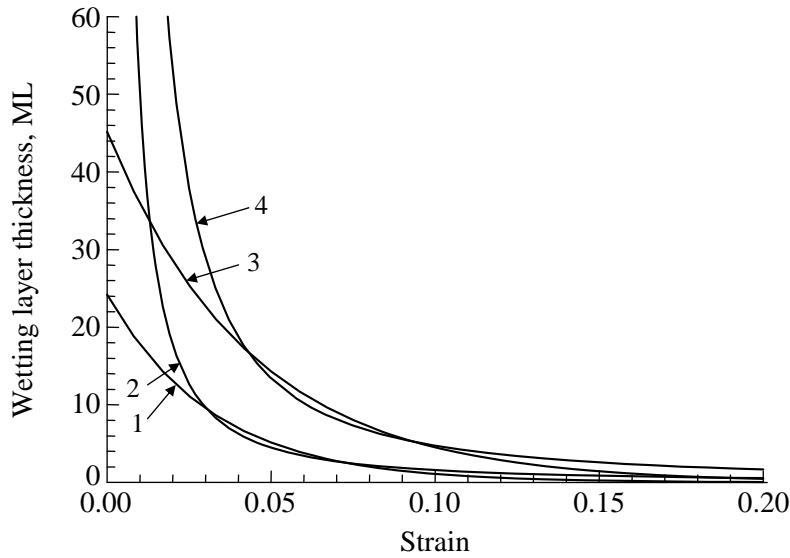


Fig. 2. Strain-dependence of the wetting layer thickness: (1) $d_{wet} = 24.181e^{-31.034\varepsilon}$ ML, $\varepsilon > 0$; (2) $d_{wet} = 0.05\varepsilon^{-3/2}$ ML, $\varepsilon > 0$; (3) $d_{wet} = 45.162e^{-23.03|\varepsilon|}$ ML, $\varepsilon < 0$; (4) $d_{wet} = 0.15|\varepsilon|^{-3/2}$ ML, $\varepsilon < 0$.

Dependence of the GaAsSbP strain-induced dots and pits total energy versus volume, calculated at $\gamma_e = 3.28 \times 10^{-4}$ J/cm², $\mu = 5.32 \times 10^5$ J/cm³, $C_{11} = 12.05 \times 10^5$ J/cm³, $C_{44} = 5.85 \times 10^5$ J/cm³, $\nu = 0.353$ and $\theta = 0.785$ (45°), is presented in Fig. 3a for different values of strain.

To attain a stable geometry, the island must first overcome the energy barrier E^* which occurs at volume V^* . Finding the maximum of energy (2), dependences of the critical energy and volume versus strain are presented in Figs. 3b and 3c, respectively. From these figures it is seen that either E^* or V^* strongly depend on the strain and dramatically decrease at the increasing of the strain, and at the critical strain of $\epsilon^* = 0.03$ the sign is changed. We assume that at $\epsilon = \epsilon^*$ the mechanism of the nucleation is changed from the growth of dots to the nucleation of pits. Clearly, at small misfit ($\epsilon < \epsilon^*$), the bulk nucleation mechanism dominates. But at $\epsilon > \epsilon^*$, when the energy barrier becomes negative as well as a larger misfit provides a low-barrier path for the formation of dislocations, the nucleation of pits becomes energetically preferable.

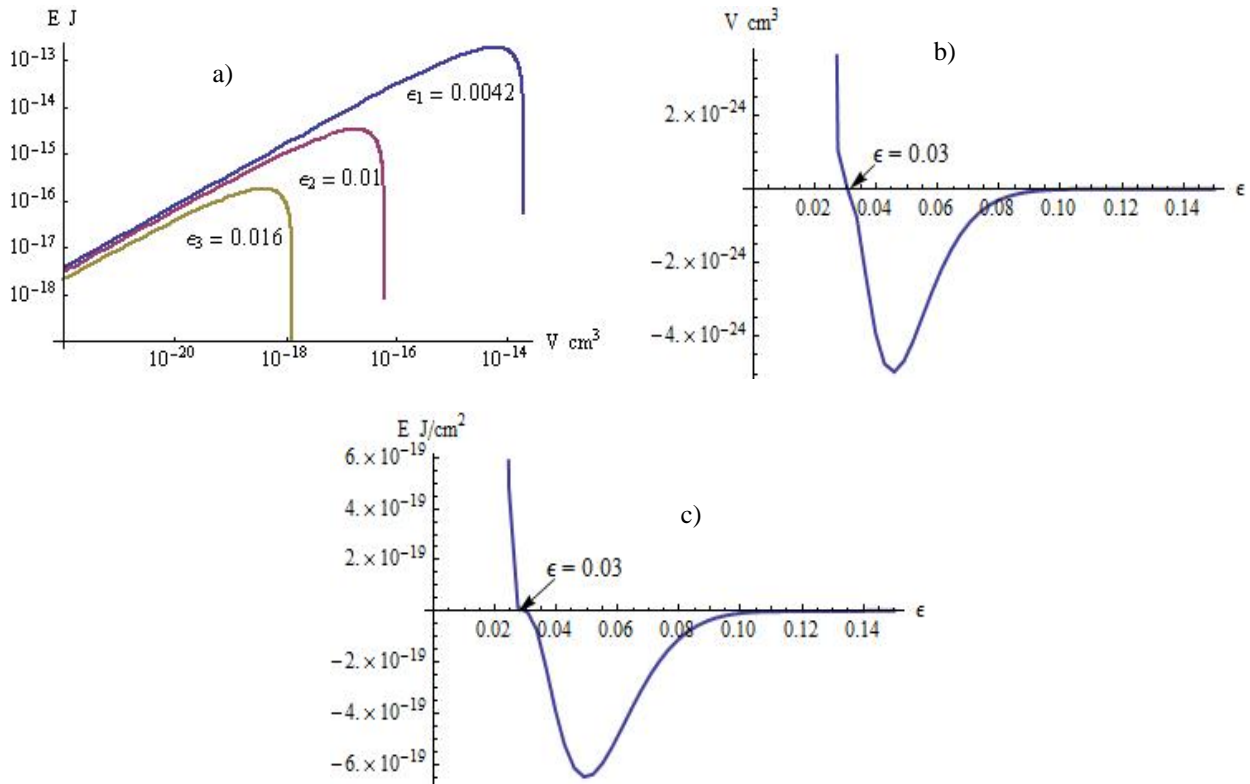


Fig. 3. a) Dependence of the GaAsSbP strain-induced islands (dots and pits) energy versus volume at different strain (1) $\epsilon_1 = 0.0042$, 2) $\epsilon_2 = 0.01$, 3) $\epsilon_2 = 0.016$; b) volume, c) critical energy.

Then, we calculated the free energy of mixing of the $\text{GaAs}_{1-x-y}\text{Sb}_x\text{P}_y$ ternary systems using the following relationship:

$$\Delta F(x, y) = \Delta H - T\Delta S, \quad (3)$$

where T is the absolute temperature and ΔH and ΔS are the enthalpy and entropy of mixing, respectively, which are determined by the following expressions [14]:

$$\begin{aligned} \Delta H(x, y) &= \varpi_{\text{GaAs}}(1-x-y) + \varpi_{\text{GaSb}}x + \varpi_{\text{GaP}}y + \alpha_{\text{GaAs-GaSb}}(1-x-y)x + \\ &+ \alpha_{\text{GaSb-GaP}}xy + \alpha_{\text{GaAs-GaP}}(1-x-y)y, \\ \Delta S(x, y) &= RT \left\{ (1-x-y) \ln(1-x-y) + x \ln x + y \ln y \right\}. \end{aligned} \quad (4)$$

Here ω is the sum of energies of interaction with the first and second nearest neighbor atoms, α the parameter of pseudobinary interaction, and R the universal gas constant [14,15]. The interaction parameter α is the characteristic index of immiscibility tension. Numerical values for ω and α parameters for GaAs–GaSb–GaP system have been taken from [14,15].

Concentration dependences of the free energy per mole for the GaAs–GaP, GaAs–GaSb, and GaSb–GaP binary systems at different temperatures in the range of 800–1200 K are shown in Fig. 4. For construction of these plots, Eq. (3) was used with ΔH and ΔS from Eq. (4).

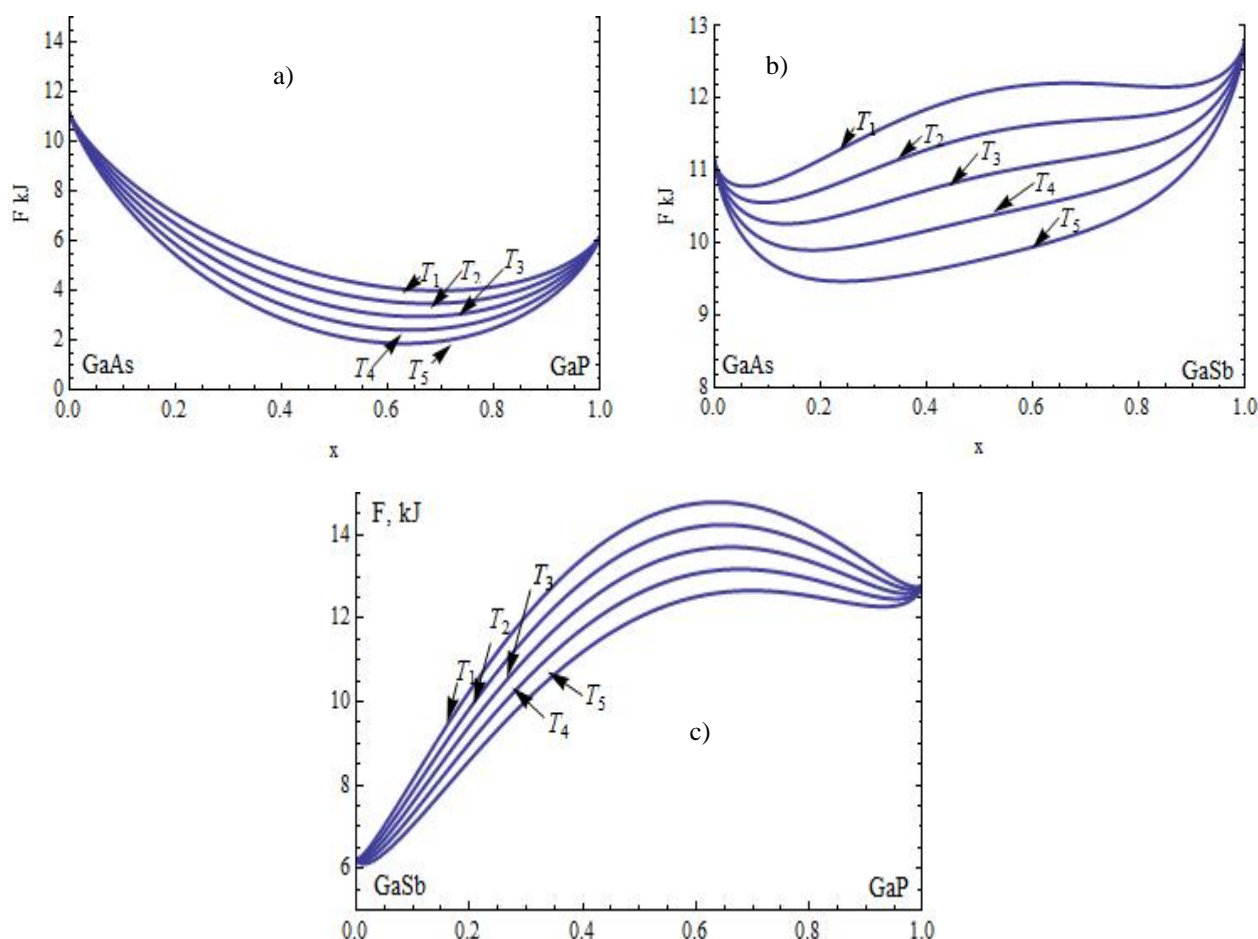


Fig. 4. Concentration dependence of the free energy for one mole of binary compounds GaAs–GaP (a), GaAs–GaSb (b), and GaSb–GaP (c) at temperatures (T_1) 800 K, (T_2) 900 K, (T_3) 1000 K, (T_4) 1100 K, and (T_5) 1200 K.

As seen from Fig. 4, in GaAs–GaP, GaAs–GaSb, and GaSb–GaP binary systems a region of immiscibility appears in GaSb–GaP system which is caused by an increase in free energy. Immiscibility gap appears also in GaAs–GaSb system but at lower temperatures. As seen, for GaAs–GaSb system at increasing temperature the maximum disappears. In systems with large difference in lattice constants high positive enthalpy of mixing can overcome the negative entropy of mixing at temperatures below critical leading to the increase in free energy. This means that in equilibrium a disordered solid solution with a composition between the binodal points shown in Fig. 5 will decay into two separate solid phases [16].

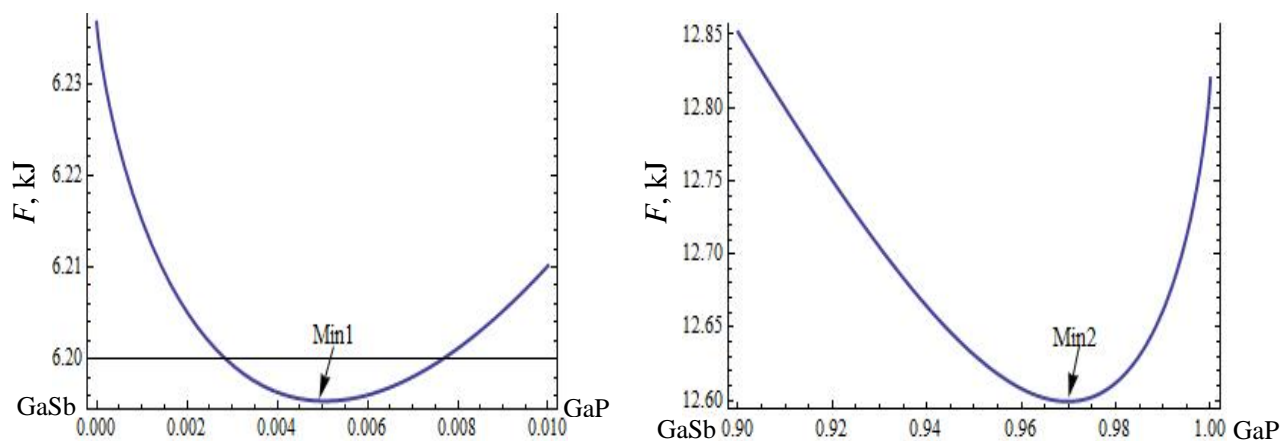


Fig. 5. Binodal points (magnified near the minima) of the curves of molar free energy shown in Fig. 4 for the GaSb–GaP system.

Schematic 3D pattern of molar free energy depending on composition of the GaAsSbP quasiternary system at $T = 800$ K and corresponding isoenergetic sections at $T = 800$ K and $T = 1200$ K are presented in Figs. 6 and 7, respectively.

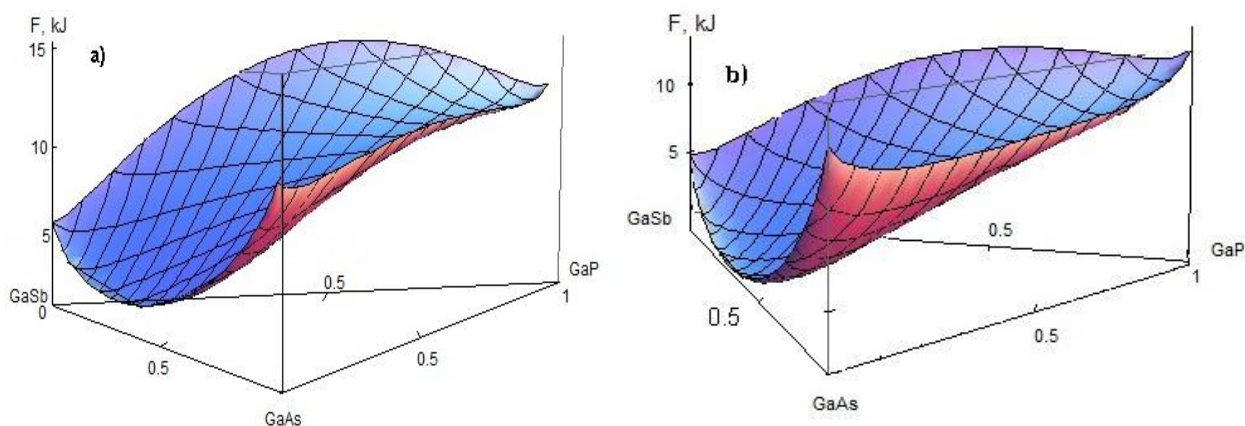


Fig. 6. Schematic 3D pattern of the molar free energy of GaAs–GaSb–GaP quasiternary material system at a) $T = 800$ K and b) $T = 1200$ K.

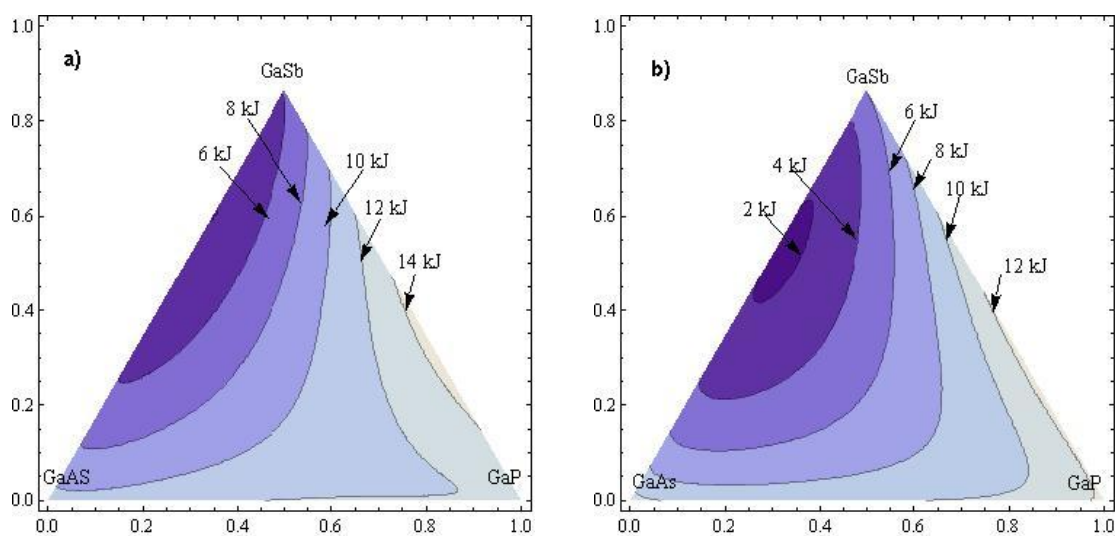


Fig. 7. Isoenergetic sections of the molar free energy of the GaAsSbP quasiternary system at the temperatures of (a) 800 K and (b) 1200 K.

Schematic pattern of the concentration triangle for one mole of GaAsSbP quasiternary material system is shown in Fig. 8. GaAsSbP solid solutions with the composition along the solid line M_0N_0 are lattice-matched with the GaAs substrate. It is shown that at $x = 0.678$ the lattice constant for GaSb $_{1-x}$ P $_x$ system is matched with the GaAs substrate. The ellipsoids mark the regions of concentrations with positive and negative signs of mismatch of lattice constants. Compositions with constant values of lattice mismatch are marked by lines and the corresponding values of deformation strain for each line are given in the appended table.

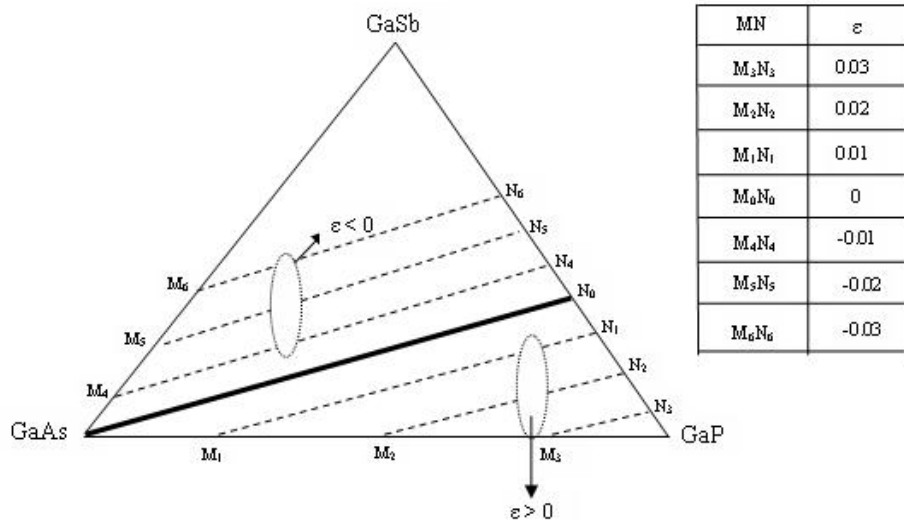


Fig. 8. Concentration triangle for the GaAsSbP quasiternary material system.

3. Conclusion

Thus, we applied the continuum model of elasticity for quantitative study of growth properties and the nucleation mechanism of QD and nanopits in GaAsSbP quasiternary material system. Calculations have shown that the sign and magnitude of the lattice mismatch parameter play an important role in growth of strained nanoobjects. We showed that in GaAsSbP quasiternary system the large mismatch leads to decreasing the critical volume and energy of QDs. We calculated critical values of the deformation strain (composition) in that system when the growth mode changes from QD nucleation to nanopit formation. The free energy of mixing for the GaAsSbP quasiternary system was calculated and studied. It was demonstrated that there is an immiscibility gap for that system, which strongly depends on temperature.

REFERENCES

1. J.Tersoff, F.K. Le Goues, Phys. Rev. Lett., **72**, 3570 (1994).
2. K.M.Gambaryan, V.M.Aroutiounian, and V.G.Harutyunyan, Infrared Phys. Techn., **54**, 114 (2011).
3. K.M.Gambaryan, Nanoscale Res. Lett., **5**, 587 (2010).
4. V.M.Aroutiounian, K.M.Gambaryan, P.G.Soukiassian, Surf. Sci., **604**, 1127 (2010).
5. C.Coster, et al., J. Appl. Phys., **98**, 126105 (2005).

6. **J.M.Ulloa, et al.**, Phys. Rev. B, **81**, 165305 (2010).
7. **J.C. DeWinter, R.E.Nahory, M.A.Pollack**, US Patent 4072544 (H01L21208), February 7, 1978.
8. **Yu.B.Bolkhovityanov, et al.**, Crystal Res. Techn., **17**, 1491 (1982).
9. **L.V.Golubev, et al.**, J. Crystal Growth, **146**, 277 (1995).
10. **R.Timm, et.al.**, Physica E, **26**, 231 (2005).
11. **J.Tersoff, F.K.LeGoues**, Phys. Rev. Letters, **72**, 3570 (1994).
12. **K.M.Gambaryan, V.M.Aroutiounian, A.K.Simonyan, L.G.Movsesyan**, J. Contemp. Phys. (Armenian Ac. Sci.), **47(4)**, 173 (2012).
13. **M.Biehl, F.Much, C.Vey**, Int. Series of Numerical Mathematics, **149**, 41 (2005).
14. **O.S.Emeljanova, S.S.Strelchenko, M.P.Usacheva**, Semiconductors, **43**, 135 (2009).
15. **K.Onabe**, NEC Res. Develop., **72**, 1 (1984).
16. **G.B.Stringfellow**, Organometallic Vapor-Phase Epitaxy: Theory and Practice, San Diego, Elsevier, 1999.